

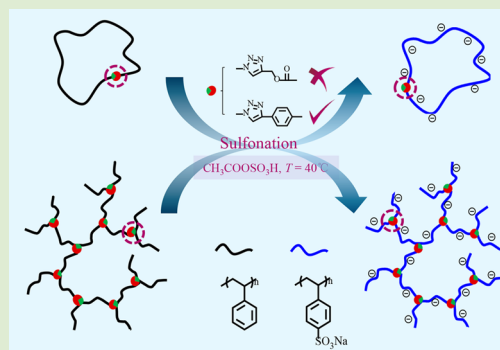
Universal Synthetic Strategy for the Construction of Topological Polystyrenesulfonates: The Importance of Linkage Stability during Sulfonation

Jianhao Si,^{†,‡} Nairong Hao,^{†,‡} Miao Zhang,[†] Siyuan Cheng,[†] Anhong Liu,[†] Lianwei Li,^{*,†,§} and Xiaodong Ye^{*,†,§}

[†]Hefei National Laboratory for Physical Sciences at the Microscale, Department of Chemical Physics, and [§]CAS Key Laboratory of Soft Matter Chemistry, University of Science and Technology of China, Hefei, Anhui 230026, China

Supporting Information

ABSTRACT: Polystyrenesulfonate (PSS), as one of the most important categories of polyelectrolytes, has received increasing attention due to its great potential in the applications of energy- and biomedical-related fields. However, most of the previous studies only focused on linear PSS and its derivatives, but little attention was paid to nonlinear topological PSSs. So far, the synthesis of nonlinear PSSs with well-defined structures is still a challenging task, and the main obstacle lies in the stability issue of functional chemical linkages during the sulfonation process of polystyrene (PS) precursors, such as the carbon–oxygen-containing linkages. Herein, by rationally designing the chemical structure of the functional linkage, we introduce a versatile and efficient strategy for the preparation of topological PSSs. Specifically, by embedding firm triazole linkages (without carbon–oxygen linkages) into the backbone structure of cyclic and hyperbranched PS precursors, the backbone and functional linkages are found to present excellent chemical stability under certain sulfonation conditions, which eventually lead to the successful preparation of cyclic and hyperbranched PSSs. By using two sets of PSS samples with varied molar masses, the scaling relations between the number of repeating units and the sedimentation coefficient are established for both linear and cyclic PSSs. We believe that our proposed synthetic strategy is universal and could be extended to the synthesis of other types of topological PSSs.



Recently, polyelectrolytes have attracted much attention due to their broad applications in the fields of biomedical research,¹ membranes,² and electrochemistry.³ Among related studies, topological polyelectrolytes with nonlinear structures were extensively investigated for the purpose of inheriting the unique properties demonstrated by neutral topological polymers.^{4–13} Namely, for cyclic polymers, the advantages, such as higher glass transition temperature,⁴ lower intrinsic viscosity,¹⁴ longer circulation half-lives,¹⁵ and enhanced micellar stability,¹⁶ are anticipated. For instance, Grayson and co-workers reported the synthesis of cyclic poly(ethylenimine) (PEI) through the hydrolysis of cyclic precursor poly(2-ethyl-2-oxazoline) and demonstrated that cyclic PEI exhibited higher gene transfection efficiency without a compromise with the cytotoxicity.⁵ Pun and co-workers synthesized cyclic poly((2-dimethylamino) ethyl methacrylate) (PDMAEMA) and found that cyclic PDMAEMA had a similar gene transfection efficiency compared with the linear counterpart but a lower cytotoxicity.⁶ Moreover, a series of topological poly(acrylic acid) (PAA) were synthesized previously.^{8–13} For example, cyclic PAA homopolymer was first synthesized by Kubo and co-workers through living anionic polymerization of *tert*-butyl acrylate followed by formic acid-assisted hydrolysis.⁸ Additionally, Szoka and co-workers expanded the synthetic

pathway by introducing atom transfer radical polymerization (ATRP) and using trifluoroacetate as the degradation agent.⁹ Their results further indicated that cyclic PEGylated PAA comb polymers had a significantly longer elimination time and a greater tumor accumulation.⁹ On the other hand, hyperbranched PAA was synthesized by Müller and co-workers through hydrolysis of a hyperbranched poly(*tert*-butyl acrylate), which was prepared from self-condensing vinyl copolymerization of *tert*-butyl acrylate and an allyl monomer with a pendent bromine group.¹¹

In addition to the categories mentioned above, polystyrenesulfonate (PSS) has also received much attention in the past decades as an irreplaceable type of polyelectrolyte, which has been widely used in ion exchange membranes,^{17,18} molecular weight standards,¹⁹ and drugs for hyperkalemia.²⁰ However, most of the related studies have only focused on linear PSS and its derivatives, but little attention was paid to the nonlinear structures, such as a well-defined hyperbranched or cyclic structure. Note that Matsushita et al. synthesized

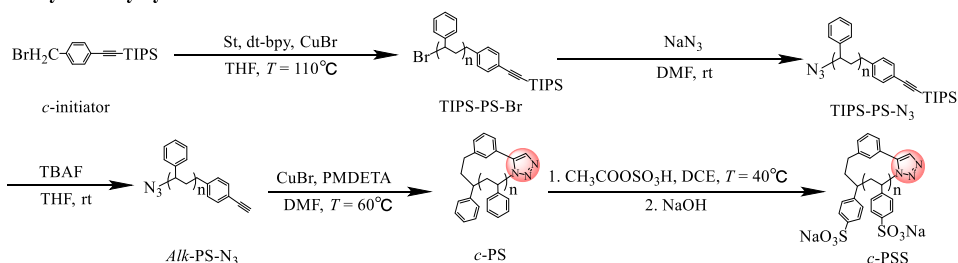
Received: April 9, 2019

Accepted: May 29, 2019

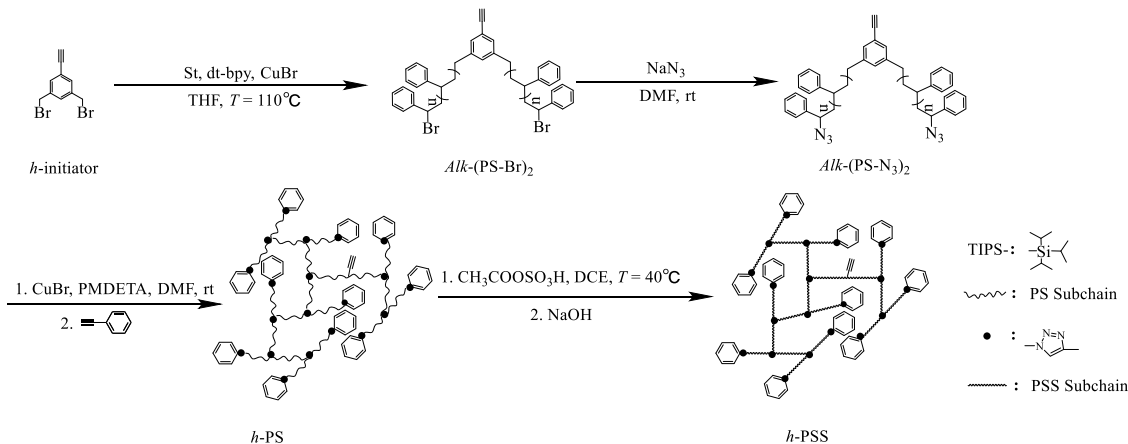
Published: June 4, 2019

Scheme 1. Schematic Synthesis of Cyclic and Long-Subchain Hyperbranched PSSs (*c*-PSS and *h*-PSS)

a. Cyclic Polystyrene Sulfonate



b. Long-subchain Hyperbranched Polystyrene Sulfonate



cyclic PSS through sulfonation of cyclic PS prepared by anionic polymerization-based ring-closure reaction and reported a direct observation of cyclic PSS chains on the surface by atomic force microscopy (AFM).²¹ Star-like PSS homo- and copolymers were also successfully synthesized through sulfonation of the PS precursors prepared by anionic polymerization through an arm-first method.^{22–24} However, despite the success of some special cases,^{21–25} these synthetic routes are not promising for other topological systems. Especially, for the star-like PSS system, it is difficult to control the exact number of arms to realize the ideal structure. Moreover, it is well-known that anionic polymerization generally suffers from poor monomer compatibility and tedious experimental preparation due to its high sensitivity to impurities. Overall, due to the poor versatility, time-consuming feature, or poor control of chain parameters, these methods are hard to extend to other systems, such as the preparation of well-defined hyperbranched polymers. Usually, for well-defined polymer architectures, the backbone length is the only chain parameter to consider for model linear and cyclic chains; for a model star-like chain, the precise control over both the arm length and the arm number is necessary; and for a model hyperbranched chain, both the subchain length between two neighboring branching points and the overall chain size must be controlled. With these requirements, ring-closure reaction, polyaddition reaction, or polycondensation reaction are the prior choices, rather than the chain-growth-based reactions. Thus, the stability issue for the existing liable linkages is the first consideration during the sulfonation process.

Nowadays, a combination of controlled radical polymerization and click chemistry has been proven to be a powerful synthetic tool for the construction of topological neutral polymers.^{26–28} Specifically, a combination of atom transfer

radical polymerization (ATRP) and copper-catalyzed azide–alkyne cycloaddition (CuAAC) was widely used for the preparation of cyclic PS and its derivatives. Unfortunately, in most of the related studies, alkyne-functional initiators with labile ester linkages were used in ATRP processes.^{12,26,29–37} Without doubt, the existence of labile ester linkages could be fatal under the harsh conditions of various sulfonation processes. Therefore, the feasibility of using C–O bond-containing initiators for the construction of topological PSSs is still questionable. We anticipate that the avoidance of introducing labile linkages into topological PS precursors is critical for the successful preparation of corresponding PSSs.

Herein, we introduce a novel synthetic scaffold for the preparation of well-defined topological PSSs with varied structures. Specifically, by embedding firm triazole-linkages (without C–O linkage) into the backbone structure of cyclic and hyperbranched PS precursors, we successfully enhanced the chemical stability of backbone and functional linkages under the harsh conditions of the sulfonation process. Moreover, the sedimentation coefficient of cyclic and linear PSSs with the number of repeating units ranging from 63–140 was briefly investigated by analytical ultracentrifugation. The scaling relations between the number of repeating units and the sedimentation coefficient were established for both linear and cyclic PSSs. The aim of this work is to provide guidance for the rational design of firm chemical linkages to construct well-defined topological PSSs.

Starting from two specially designed initiators bearing alkyne and bromine functional groups, but without labile linkages, such as the carbon–oxygen (C–O) linkage, well-defined cyclic and hyperbranched polystyrenes could be synthesized. The synthetic route is shown in Scheme S1 and the ¹H NMR spectra of the initiators and related content are shown in Figures S1 and S2. The calculated ratios of the integral areas

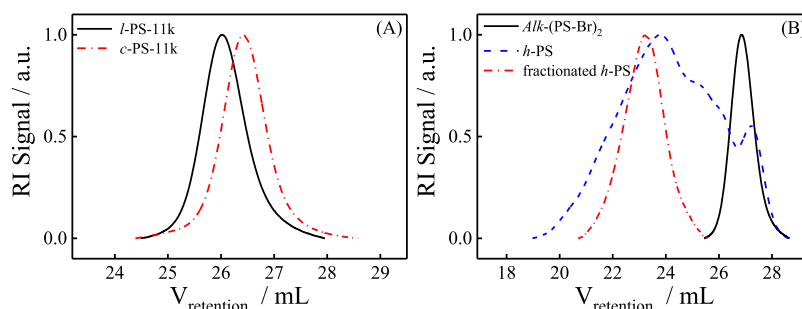


Figure 1. (A) GPC curves of the key precursors *l*-PS-11k (black solid line) and *c*-PS-11k (red dash dotted line) for the preparation of *c*-PSS. (B) GPC curves of the key precursors *Alk*-(PS-Br)₂ (black solid line), fractionated *h*-PS (red dash dotted line) and unfractionated *h*-PS (blue dashed line) for the preparation of *h*-PSS.

(A) for different protons from initiators ($A_a/A_b/A_c/A_d = 21/2/2/2$ for *c*-initiator and $A_e/A_f/A_g/A_h = 1/2/1/4$ for *h*-initiator) are consistent with the theoretical ones, indicating the successful synthesis of initiators. As shown in Scheme 1, two precursors, that is, TIPS-PS-Br with one alkyne and one bromine and *Alk*-(PS-Br)₂ with two bromines and one alkyne group, could be first obtained via the polymerization of styrene. After the azidation and deprotection process, they could be further converted into alkyne/azide functionalized *Alk*-(PS-N₃)₂ (*l*-PS) and *Alk*-(PS-N₃)₂. One of the two key neutral precursors, cyclic polystyrene (*c*-PS), could be obtained via the intramolecular cyclization of *l*-PS through CuAAC “click” reaction in a dilute solution. Similarly, the other key neutral precursor, long-subchain hyperbranched polystyrene (*h*-PS), could be obtained via the interchain “click” coupling of *Alk*-(PS-N₃)₂ in semidilute/concentrated solution.³⁸ Finally, cyclic and hyperbranched polystyrene sulfonate (*c*-PSS and *h*-PSS) could be prepared via the sulfonation of their neutral precursors, cyclic and hyperbranched polystyrenes (*c*-PS and *h*-PS).

Experimentally, *l*-PS was prepared through ATRP with the designed initiator (*c*-initiator) and with a low polydispersity and then converted to *c*-PS. Figure 1A shows the GPC curves for *c*-PS and *l*-PS, where the number average molar mass (M_n) for *l*-PS-11k is $\sim 1.12 \times 10^4$ g/mol. Clearly, a significant shift to a higher retention time is observed for the cyclized product *c*-PS-11k due to its much smaller hydrodynamic volume compared with the linear counterpart (*l*-PS-11k). The GPC curves for other sets of *c*-PS and *l*-PS with a M_n of 6.6×10^3 g/mol and 1.46×10^4 g/mol can be found in Figure S3. The ratios of peak molar masses of cyclic *c*-PS and linear *l*-PS samples are ~ 0.77 , which agrees well with the reported values in previous studies.^{25,39} Moreover, the accurate molar masses of cyclic and linear products obtained by light-scattering detector are almost the same (Table 1), which indicates the discrepancy between the apparent peak molar masses is attributed to the restriction of the cyclic topology. The GPC characterization results for *Alk*-(PS-Br)₂ and *h*-PS before and after fractionated precipitation are shown in Figure 1B. For *Alk*-(PS-Br)₂, a narrowly distributed GPC curve is observed, whereas for unfractionated *h*-PS, the GPC curve gets much broader after the interchain “click” coupling process. After fractional precipitation, *h*-PS with moderate polydispersity (fractionated *h*-PS, $M_n \sim 7.57 \times 10^4$ g/mol) was obtained.

In addition to GPC characterization, the structural details for cyclic and hyperbranched neutral precursors were also confirmed by ¹H NMR (Figures S4 and S6) and Fourier-transform infrared (FT-IR) spectroscopy (Figures S5 and S7).

Table 1. Gel Permeation Chromatography Data for Linear, Cyclic, and Hyperbranched PS Samples

samples	M_n (g/mol)	M_w (g/mol)	M_w/M_n	M_w, MALLS (g/mol)	$M_{p,c}/M_{p,l}$
<i>l</i> -PS-7k	6600	7270	1.10	7790	0.76
<i>c</i> -PS-7k	5230	5810	1.11	7950	
<i>l</i> -PS-11k	11120	12160	1.09	11490	0.77
<i>c</i> -PS-11k	8360	9960	1.19	11460	
<i>l</i> -PS-15k	14610	15650	1.07	14720	0.77
<i>c</i> -PS-15k	10960	12330	1.12	14800	
<i>Alk</i> -(PS-Br) ₂	8290	9200	1.11	9280	
<i>h</i> -PS	22000	93000	4.23	200200	
fractionated <i>h</i> -PS	75700	99500	1.31	187700	

Briefly, combined evidence based on the disappearance of the characteristic peak for azide group at 2100 cm^{-1} (Figures S5 and S7), the shift of the signal for the methine proton next to the azide group, and the appearance of the signal for the triazole ring (Figures S4 and S6) signify the high coupling efficiency between azide and alkyne groups during click reaction. Overall, the characterization results demonstrate that the ATRP polymerization, intrachain cyclization and interchain coupling processes were carried out in a controlled manner, which led to the successful preparation of key precursors, that is, *c*-PSs with varied molar masses and fractionated *h*-PS with low polydispersity. The details for their molecular information are summarized in Table 1.

Next, all the monodispersed neutral precursors in the present work were sulfonated using “acetyl sulfate” method for 12 h, and then *c*-PSSs and *h*-PSS were obtained.⁴⁰ Figure 2A and Figure 2B shows that the normalized sedimentation coefficient distributions for *c*-PS-11k and *l*-PS-11k before and after sulfonation. Before sulfonation, sedimentation coefficient (s) of *c*-PS-11k (1.49 S) is larger than that of *l*-PS-11k (1.31 S) due to its smaller hydrodynamic size. After sulfonation (Figure 2B), *c*-PSS-11k still exhibits a larger s (2.55 S) compared with *l*-PSS-11k (2.28 S) in aqueous solutions and the weight-average molar masses of *c*-PSS-11k and *l*-PSS-11k measured by analytical ultracentrifuge are close to each other, which clearly demonstrates the successful synthesis of cyclic PSS. Moreover, the average hydrodynamic radius of *c*-PSS-11k ($\langle R_h \rangle = 2.81 \text{ nm}$) is indeed smaller than that of the linear counterpart *l*-PSS-11k ($\langle R_h \rangle = 3.61 \text{ nm}$) and the frictional ratio (f/f_0) of *c*-PSS-11k is 1.69, which is smaller than that of *l*-PSS-11k ($f/f_0 = 2.05$), further indicating the more symmetric structure of cyclic PSS. Similar results were observed for other *c*-PSS samples with different molar masses (Figures S8 and S9 and Table S1).

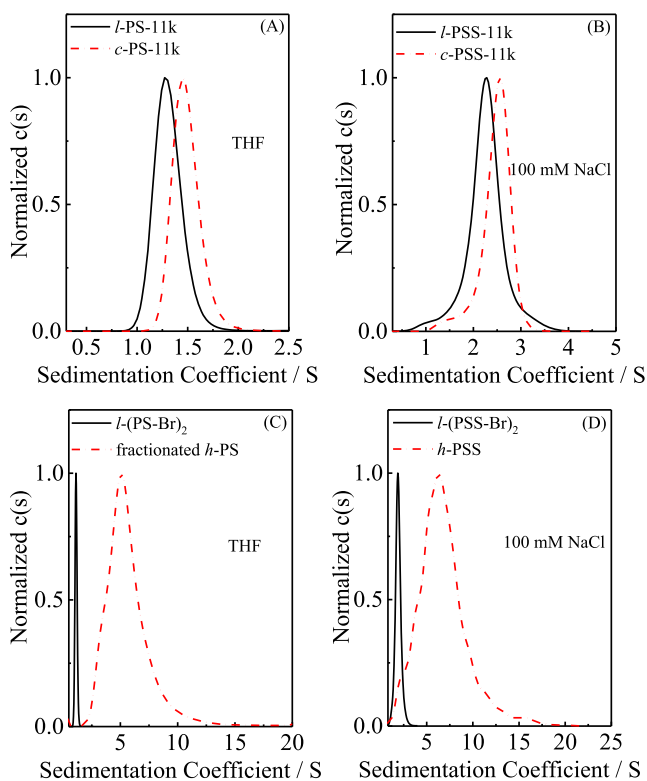


Figure 2. Normalized sedimentation coefficient distributions $c(s)$ of (A) c -PS-11k (red dash dotted line) sample and its linear precursor l -PS-11k (black solid line) in THF, (B) c -PSS-11k (red dash dotted line) sample and its linear counterpart l -PSS-11k (black solid line) in 100 mM NaCl aqueous solutions, (C) fractionated h -PS (red dash dotted line) and corresponding macromonomer l -(PS-Br)₂ (black solid line) in THF, and (D) sulfonation product of fractionated h -PS (red dash dotted line) and corresponding macromonomer l -(PS-Br)₂ (black solid line) in 100 mM NaCl aqueous solutions.

For h -PS, Figure 2C,D shows that the sedimentation coefficients of fractionated h -PS and h -PSS are much larger than those of macromonomer counterparts in organic or aqueous solutions, apparently due to the much higher molar mass.

It is well-known that for topological polymers, both sedimentation coefficient and diffusion coefficient at infinite dilution are scaled to the molar mass (M_w) as $s_0 = K_s M_w^a$ and $D_0 = K_D M_w^{-\beta}$, where $a + \beta = 1$. These two scaling indexes could give the information about the chain conformation. For a compact sphere, a random coil, and a rigid rod, a is 0.67, 0.4–0.5, and 0.15, respectively.⁴¹ We know that sedimentation coefficient s at a finite polymer concentration (C_p) is related to s_0 by the equation $s = s_0(1 - k_s C_p)$, where k_s is the sedimentation concentration coefficient, which reflects the interaction between polymer chains and decreases with the decreasing molar mass.^{42,43} In this study, k_s is measured to be 0.04 and 0.017 for l -PSS-15k and c -PSS-15k (Figure S10), respectively, indicating that the concentration dependence of s is weak for both l -PSS and c -PSS. Therefore, the value of s at $C_p = 0.25$ mg/mL was used to substitute s_0 . Figure 3 shows that the sedimentation coefficients of l -PSS and c -PSS scale to the number of repeating units as $s_l = (0.34 \pm 0.06)N^{0.41 \pm 0.03}$ and $s_c = (0.43 \pm 0.03)N^{0.38 \pm 0.01}$, indicating l -PSS adopts a similar conformation with c -PSS, although for each pair of samples, the s of c -PSS is always larger than that of l -PSS. Note that Amis and co-workers also found that the values of scaling

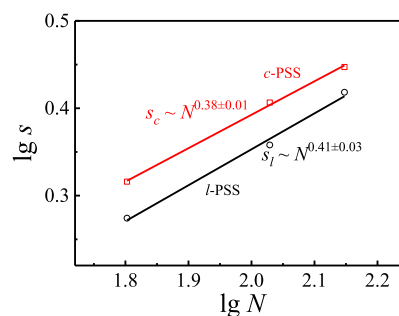


Figure 3. Number of repeating units dependence of sedimentation coefficient of linear and cyclic PSSs (l -PSS and c -PSS).

index β for linear and cyclic poly(2-vinylpyridine) (P2VP) in 0.23 M HCl were similar to each other, namely, $D_0^c \sim M_w^{-0.52}$ for cyclic P2VP and $D_0^l \sim M_w^{-0.53}$ for the linear counterpart.⁷ Moreover, for linear PSSs, the fitted scaling index a_l is quite close to the value reported by Zhang and co-workers,⁴⁴ which indicates that both l -PSS and c -PSS adopt a random coil conformation rather than a rigid rod in 100 mM NaCl aqueous solutions since the electrostatic interaction is well shielded.

Prior to the preparation of topological PSSs, the linkage stability must be the major concern since it is quite a harsh postmodification process for the sulfonation reaction. Therefore, choosing a robust linkage and appropriate sulfonation condition must be the main consideration. Herein, in order to test the stability issue of the triazole ring linkage during the sulfonation process, a diblock polystyrene sample (PS-triazole-PS) with a triazole ring linkage in the chain center was synthesized as a model sample. The synthetic details can be found in Scheme S2. As shown in Figure 4A, two representative sulfonation methods were used in experiments. In method I,⁴⁵ PS-triazole-PS powder was dissolved into an excess amount of 97% concentrated sulfuric acid and kept stirring at 90 °C for 3 h. In method II, acetyl sulfate was used as the sulfonation reagent, instead of concentrated sulfuric acid, and accordingly, a milder condition (in dichloroethane at 40 °C for 12 h) was used.⁴⁰

Figure 4B shows the normalized sedimentation coefficient distributions $c(s)$ for PS-triazole-PS diblock and its linear precursor l -PSS-3k. The sedimentation coefficient s of PS-triazole-PS is found to rise to 1.09 S compared with that of the linear precursor (0.91 S), indicating the successful synthesis of the diblock polymer. The characterization results for method I (“hard” sulfonation) and method II (“soft” sulfonation) are shown in Figure 4C,D. For method I, the result shows that s of the sulfonated products of PS-triazole-PS and l -PSS-3k, that is, PSS-triazole-PSS and l -PSS-3k, are pretty close to each other (Figure 4C). Such an observation unambiguously demonstrates that the PS-triazole-PS diblock suffered degradation and degraded to half due to the instability of triazole linkage during the “hard” sulfonation process (method I). Moreover, both distribution curves show shoulder peaks at large- s regimes, demonstrating the formation of interchain cross-linked product under such condition. Figure 4D shows the result for “soft” sulfonation method (method II). Both PSS-triazole-PSS and l -PSS-3k display unimodal distributions. More importantly, s of PSS-triazole-PSS is much higher than that of l -PSS-3k, indicating that triazole ring is intact under this mild sulfonation condition. The experimental result clearly demonstrates that the stability of firm triazole linkage could be guaranteed only under mild sulfonation condition.

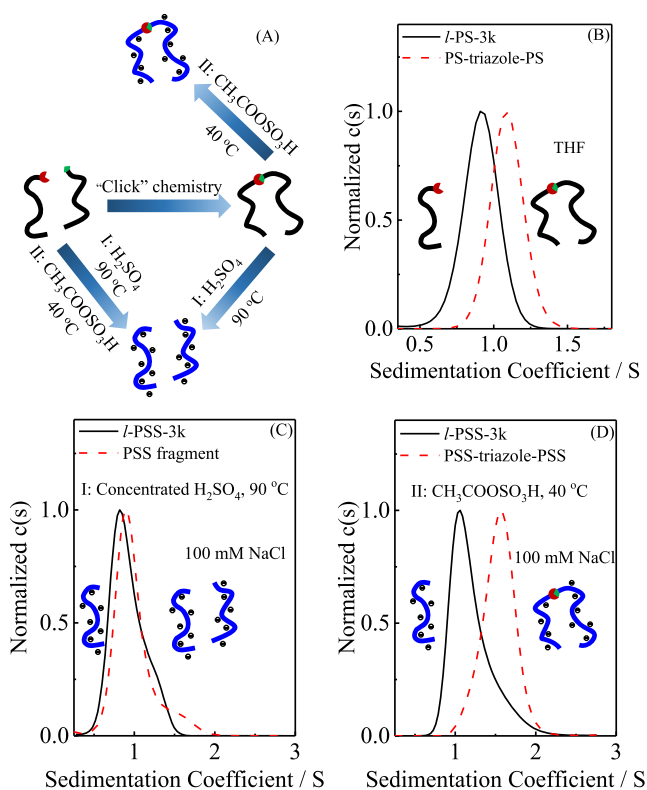


Figure 4. (A) Schematic for the testing of chemical stability of triazole linkage during two representative sulfonation processes by using a diblock PS-triazole-PS containing a triazole ring linkage as the model sample. Method I: concentrated sulfuric acid at $T = 90\text{ }^{\circ}\text{C}$ for 3 h; Method II: acetyl sulfate in dichloroethane at $T = 40\text{ }^{\circ}\text{C}$ for 12 h. (B) Normalized sedimentation coefficient distributions $c(s)$ of *l*-PS-3k (black solid line) and the corresponding dimer PS-triazole-PS (red dashed dotted line) in THF, (C) normalized $c(s)$ of the corresponding sulfonating product of *l*-PS-3k (black solid line) and the dimeric product PS-triazole-PS (red dashed dotted line) in 100 mM NaCl using method I, and (D) normalized $c(s)$ of the corresponding sulfonating product of *l*-PS-3k (black solid line) and the dimeric product PS-triazole-PS (red dashed dotted line) in 100 mM NaCl using method II.

In addition to the triazole ring linkage, it is also intriguing to explore the stability of ester linkage during sulfonation process. Since the introduction of synthetic methodology based on the combination of ATRP and CuAAC for the preparation of cyclic homo- and copolymers by Grayson and co-workers,²⁶ numerous topological neutral (co)polymers have been synthesized by this synthetic protocol.^{29–37} Among most of related studies, ester linkages were embedded into the backbone structures of cyclic products, but the stability issue of ester linkage has not been addressed yet. Thus, a control experiment was further carried out to test the stability of ester linkage during sulfonation process, and the result will be beneficial for the rational design of synthetic protocol for the preparation of well-defined topological polyelectrolytes under harsh postpolymerization modification processes. For this purpose, a polystyrene model sample (PS-ester-PS) with two ester linkages in the chain center was synthesized, as shown in Scheme S2. We found that the ester linkage was cleaved, even during the “soft” sulfonation condition. Figure S11 summarizes the normalized $c(s)$ for PS-ester-PS before and after sulfonation. For comparison, the result for a linear PS sample (*l*-PS-4k) is also shown. Before sulfonation, s of PS-ester-PS is

higher than that of *l*-PS-4k, but after sulfonation, s of the corresponding sulfonation product is smaller than that of *l*-PSS-4k, clearly indicating the degradation of PS-ester-PS during the sulfonation process. Obviously, the result suggests that the oxygen-containing linkages will suffer stability issues even when they are exposed to a “soft” sulfonation condition, and the use of C–O linkage-containing initiators for the preparation of topological PSS is not feasible.

For further optimizing the sulfonation condition, the effect of sulfonation time (t) was studied under “soft” sulfonation condition (method II). The degree of sulfonation for *l*-PS-4k was determined by ¹H NMR by calculating the ratio of the integral areas between the protons from backbone and aromatic ring. Time dependence of the degree of sulfonation is plotted in Figure S12. The degree of sulfonation increases dramatically to 75% at $t = 7$ h and subsequently reaches to 92% at $t = 12$ h, which is comparable with the commercialized product.⁴⁶ Eventually, the degree of sulfonation increases to ~94% at $t = 18$ h. In this study, all PS precursors were sulfonated by method II for 12 h to suppress possible side reactions.

In conclusion, we have introduced a versatile synthetic pathway toward the preparation of polystyrenesulfonates with different topological structures. Using designed initiators without C–O bond-containing groups, cyclic and hyperbranched polystyrenes with triazole rings as the only linkage were successfully synthesized through the combination of atom transfer radical polymerization and copper-catalyzed azide–alkyne cycloaddition, which have proved to have great stability during the sulfonation process using acetyl sulfate as the sulfonating reagent. Subsequent analytical ultracentrifugation characterization further demonstrates the cyclic and hyperbranched structure of the sulfonating product, as indicated by the higher sedimentation coefficients induced by a smaller size for cyclic structure or higher molar mass for a hyperbranched product. The scaling relation between the sedimentation coefficient and the number of repeating units indicates that both *l*-PSS and *c*-PSS adopt a random coil conformation in aqueous solutions. Our research supplies a novel and accessible way for the synthesis of polystyrenesulfonate with different topologies. Moreover, this synthetic scaffold could provide an accessible way to investigate the solution behavior of topological polyelectrolytes. Further investigations on the effect of chain topology on the complexation between polyelectrolytes are underway in our laboratory.

■ ASSOCIATED CONTENT

📄 Supporting Information

The Supporting Information is available free of charge on the ACS Publications website at DOI: 10.1021/acsmacrolett.9b00260.

Experimental details, GPC results, FT-IR and ¹H NMR spectra of the neutral precursors, AUC results of cyclic PSSs with varied molar masses, figures for the stability test results of ester linkage, and the time dependence of the degree of sulfonation (PDF)

■ AUTHOR INFORMATION

Corresponding Authors

*E-mail: xdye@ustc.edu.cn.

*E-mail: llw@mail.ustc.edu.cn.

ORCID 

Lianwei Li: 0000-0002-1996-6046

Xiaodong Ye: 0000-0003-2143-1726

Author Contributions

[‡]These authors contributed equally to this work.

Notes

The authors declare no competing financial interest.

ACKNOWLEDGMENTS

The financial support of the National Natural Scientific Foundation of China (NNSFC) Projects (21674107, 51773192, and 21774116) and the Fundamental Research Funds for the Central Universities (WK2340000066) are gratefully acknowledged.

REFERENCES

- (1) Boudou, T.; Crouzier, T.; Ren, K. F.; Blin, G.; Picart, C. Multiple Functionalities of Polyelectrolyte Multilayer Films: New Biomedical Applications. *Adv. Mater.* **2010**, *22*, 441–467.
- (2) Smitha, B.; Sridhar, S.; Khan, A. A. Polyelectrolyte Complexes of Chitosan and Poly(acrylic acid) As Proton Exchange Membranes for Fuel Cells. *Macromolecules* **2004**, *37*, 2233–2239.
- (3) Wee, G.; Larsson, O.; Srinivasan, M.; Berggren, M.; Crispin, X.; Mhaisalkar, S. Effect of the Ionic Conductivity on the Performance of Polyelectrolyte-Based Supercapacitors. *Adv. Funct. Mater.* **2010**, *20*, 4344–4350.
- (4) Hossain, M. D.; Lu, D. R.; Jia, Z. F.; Monteiro, M. J. Glass Transition Temperature of Cyclic Stars. *ACS Macro Lett.* **2014**, *3*, 1254–1257.
- (5) Cortez, M. A.; Godbey, W. T.; Fang, Y.; Payne, M. E.; Cafferty, B. J.; Kosakowska, K. A.; Grayson, S. M. The Synthesis of Cyclic Poly(ethylene imine) and Exact Linear Analogues: An Evaluation of Gene Delivery Comparing Polymer Architectures. *J. Am. Chem. Soc.* **2015**, *137*, 6541–6549.
- (6) Wei, H.; Chu, D. S. H.; Zhao, J.; Pahang, J. A.; Pun, S. H. Synthesis and Evaluation of Cyclic Cationic Polymers for Nucleic Acid Delivery. *ACS Macro Lett.* **2013**, *2*, 1047–1050.
- (7) Hodgson, D. F.; Amis, E. J. Dilute-Solution Behavior of Cyclic and Linear Polyelectrolytes. *J. Chem. Phys.* **1991**, *95*, 7653–7663.
- (8) Kubo, M.; Nishigawa, T.; Uno, T.; Itoh, T.; Sato, H. Cyclic Polyelectrolyte: Synthesis of Cyclic Poly(acrylic acid) and Cyclic Potassium Polyacrylate. *Macromolecules* **2003**, *36*, 9264–9266.
- (9) Chen, B.; Jerger, K.; Frechet, J. M. J.; Szoka, F. C. The Influence of Polymer Topology on Pharmacokinetics: Differences Between Cyclic and Linear PEGylated Poly(acrylic acid) Comb Polymers. *J. Controlled Release* **2009**, *140*, 203–209.
- (10) Chen, F. G.; Liu, G. M.; Zhang, G. Z. Synthesis of Cyclic Polyelectrolyte via Direct Copper(I)-catalyzed Click Cyclization. *J. Polym. Sci., Part A: Polym. Chem.* **2012**, *50*, 831–835.
- (11) Mori, H.; Seng, D. C.; Lechner, H.; Zhang, M. F.; Müller, A. H. E. Synthesis and Characterization of Branched Polyelectrolytes. 1. Preparation of Hyperbranched Poly(acrylic acid) via Self-Condensing Atom Transfer Radical Copolymerization. *Macromolecules* **2002**, *35*, 9270–9281.
- (12) Kim, B. S.; Gao, H.; Argun, A.; Matyjaszewski, K.; Hammond, P. T. All-Star Polymer Multilayers as pH-Responsive Nanofilms. *Macromolecules* **2009**, *42*, 368–375.
- (13) Furukawa, T.; Ishizu, K. Synthesis and Viscoelastic Behavior of Multiarm Star Polyelectrolytes. *Macromolecules* **2005**, *38*, 2911–2917.
- (14) Jeong, Y.; Jin, Y.; Chang, T.; Uhlik, F.; Roovers, J. Intrinsic Viscosity of Cyclic Polystyrene. *Macromolecules* **2017**, *50*, 7770–7776.
- (15) Nasongkla, N.; Chen, B.; Macaraeg, N.; Fox, M. E.; Frechet, J. M. J.; Szoka, F. C. Dependence of Pharmacokinetics and Biodistribution on Polymer Architecture: Effect of Cyclic versus Linear Polymers. *J. Am. Chem. Soc.* **2009**, *131*, 3842–3843.
- (16) Honda, S.; Yamamoto, T.; Tezuka, Y. Tuneable Enhancement of the Salt and Thermal Stability of Polymeric Micelles by Cyclized Amphiphiles. *Nat. Commun.* **2013**, *4*, 1574–1583.
- (17) Smitha, B. Synthesis and Characterization of Proton Conducting Polymer Membranes for Fuel Cells. *J. Membr. Sci.* **2003**, *225*, 63–76.
- (18) Rikukawa, M.; Sanui, K. Proton-conducting Polymer Electrolyte Membranes Based on Hydrocarbon Polymers. *Prog. Polym. Sci.* **2000**, *25*, 1463–1502.
- (19) Brown, D. W.; Lowry, R. E. Molecular-Weight Standards from Sulfonation of Polystyrene. *J. Polym. Sci., Polym. Chem. Ed.* **1979**, *17*, 1039–1046.
- (20) Scherr, L.; Ogden, D. A.; Mead, A. W.; Spritz, N.; Rubin, A. L. Management of Hyperkalemia with a Cation-exchange Resin. *N. Engl. J. Med.* **1961**, *264*, 115–119.
- (21) Kawaguchi, D.; Nishu, T.; Takano, A.; Matsushita, Y. Direct Observation of an Isolated Cyclic Sodium Poly(styrenesulfonate) Molecule by Atomic Force Microscopy. *Polym. J.* **2007**, *39*, 271–275.
- (22) Heinrich, M.; Rawiso, M.; Zilliox, J. G.; Lesieur, P.; Simon, J. P. Small-angle X-ray Scattering from Salt-free Solutions of Star-branched Polyelectrolytes. *Eur. Phys. J. E* **2001**, *4*, 131–142.
- (23) Yang, J. C.; Mays, J. W. Synthesis and Characterization of Neutral/Ionic Block Copolymers of Various Architectures. *Macromolecules* **2002**, *35*, 3433–3438.
- (24) Boue, F.; Combet, J.; Deme, B.; Heinrich, M.; Zilliox, J. G.; Rawiso, M. SANS from Salt-Free Aqueous Solutions of Hydrophilic and Highly Charged Star-Branched Polyelectrolytes. *Polymers* **2016**, *8*, 228–347.
- (25) Takano, A.; Kushida, Y.; Aoki, K.; Masuoka, K.; Hayashida, K.; Cho, D.; Kawaguchi, D.; Matsushita, Y. HPLC Characterization of Cyclization Reaction Product Obtained by End-to-End Ring Closure Reaction of a Telechelic Polystyrene. *Macromolecules* **2007**, *40*, 679–681.
- (26) Laurent, B. A.; Grayson, S. M. An Efficient Route to Well-Defined Macrocyclic Polymers via “Click” Cyclization. *J. Am. Chem. Soc.* **2006**, *128*, 4238–4239.
- (27) Qiu, X. P.; Tanaka, F.; Winnik, F. M. Temperature-Induced Phase Transition of Well-Defined Cyclic Poly(*N*-isopropylacrylamide)s in Aqueous Solution. *Macromolecules* **2007**, *40*, 7069–7071.
- (28) Stamenović, M. M.; Espeel, P.; Baba, E.; Yamamoto, T.; Tezuka, Y.; Du Prez, F. E. Straightforward Synthesis of Functionalized Cyclic Polymers in High Yield via RAFT and Thiolactone–disulfide Chemistry. *Polym. Chem.* **2013**, *4*, 184–193.
- (29) Hadjichristidis, N.; Iatrou, H.; Pitsikalis, M.; Mays, J. Macromolecular Architectures by Living and Controlled/Living Polymerizations. *Prog. Polym. Sci.* **2006**, *31*, 1068–1132.
- (30) Gao, H. F.; Matyjaszewski, K. Synthesis of Star Polymers by a Combination of ATRP and the “Click” Coupling Method. *Macromolecules* **2006**, *39*, 4960–4965.
- (31) Eugene, D. M.; Grayson, S. M. Efficient Preparation of Cyclic Poly(methyl acrylate)-block-poly(styrene) by Combination of Atom Transfer Radical Polymerization and Click Cyclization. *Macromolecules* **2008**, *41*, 5082–5084.
- (32) Lonsdale, D. E.; Monteiro, M. J. Various Polystyrene Topologies Built from Tailored Cyclic Polystyrene via CuAAC Reactions. *Chem. Commun.* **2010**, *46*, 7945–7947.
- (33) Li, L. W.; He, C.; He, W. D.; Wu, C. Formation Kinetics and Scaling of “Defect-Free” Hyperbranched Polystyrene Chains with Uniform Subchains Prepared from Seesaw-Type Macromonomers. *Macromolecules* **2011**, *44*, 8195–8206.
- (34) Jiang, X. B.; Shi, Y.; Zhu, W.; Chen, Y. M.; Xi, F. Synthesis of Mikto-topology Star Polymer Containing One Cyclic Arm. *J. Polym. Sci., Part A: Polym. Chem.* **2012**, *50*, 4239–4245.
- (35) Lee, T.; Oh, J.; Jeong, J.; Jung, H.; Huh, J.; Chang, T.; Paik, H. J. Figure-Eight-Shaped and Cage-Shaped Cyclic Polystyrenes. *Macromolecules* **2016**, *49*, 3672–3680.
- (36) Xu, J.; Ye, J.; Liu, S. Y. Synthesis of Well-Defined Cyclic Poly(*N*-isopropylacrylamide) via Click Chemistry and Its Unique

Thermal Phase Transition Behavior. *Macromolecules* **2007**, *40*, 9103–9110.

(37) Gao, L.; Oh, J.; Tu, Y.; Chang, T. Preparation of Low Molecular Weight Cyclic Polystyrenes with High Purity via Liquid Chromatography at the Critical Condition. *Polymer* **2018**, *135*, 279–284.

(38) He, C.; Li, L. W.; He, W. D.; Jiang, W. X.; Wu, C. Click” Long Seesaw-Type A~B~A Chains Together into Huge Defect-Free Hyperbranched Polymer Chains with Uniform Subchains. *Macromolecules* **2011**, *44*, 6233–6236.

(39) Roovers, J.; Toporowski, P. M. Synthesis of High Molecular-Weight Ring Polystyrenes. *Macromolecules* **1983**, *16*, 843–849.

(40) Makowski, H. S.; Lundberg, R. D.; Singhal, G. H. Flexible Polymeric Compositions Comprising a Normally Plastic Polymer Sulfonated to About 0.2 to About 10 mol % Sulfonate. U.S. Patent 3870841, 1975.

(41) Harding, S. E. On the Hydrodynamic Analysis of Macromolecular Conformation. *Biophys. Chem.* **1995**, *55*, 69–93.

(42) Rowe, A. J. The Concentration Dependence of Transport Processes: A General Description Applicable to the Sedimentation, Translational Diffusion, and Viscosity Coefficients of Macromolecular Solutes. *Biopolymers* **1977**, *16*, 2595–2611.

(43) Solovyova, A.; Schuck, P.; Costenaro, L.; Ebel, C. Non-ideality by Sedimentation Velocity of Halophilic Malate Dehydrogenase in Complex Solvents. *Biophys. J.* **2001**, *81*, 1868–1880.

(44) Luo, Z. L.; Zhang, G. Z. Sedimentation of Polyelectrolyte Chains in Aqueous Solutions. *Macromolecules* **2010**, *43*, 10038–10044.

(45) Coughlin, J. E.; Reisch, A.; Markarian, M. Z.; Schlenoff, J. B. Sulfonation of Polystyrene: Toward the “Ideal” Polyelectrolyte. *J. Polym. Sci., Part A: Polym. Chem.* **2013**, *51*, 2416–2424.

(46) Luo, Z. L.; Zhang, G. Z. Sedimentation of Polyelectrolyte Chains in Solutions: From Dilute to Semidilute. *Polymer* **2011**, *52*, 5846–5850.